



# Effect of incident intensity and operating temperature on the conversion efficiency of triple-junction GaAs cells for wireless laser power transmission

Jingyang Han\*, Jian Zhang, Shangbin Bai\*

Jiyang College, Zhejiang A&F University, Hangzhou, 311300, China

\*Corresponding author: Jingyang Han1\*, jingyanghan@163.com

\*Co-corresponding authors: Shangbin Bai1\*, bshbin@21cn.com

## Introduction

Unmanned aerial vehicles (UAVs) have been widely applied in military, commercial and civilian fields, yet their flight endurance is severely constrained by the limited capacity of onboard batteries. Laser wireless power transfer (LWPT) offers an effective solution to extend UAV endurance, while the actual electrical-to-electrical efficiency of current LWPT systems is only around 15%. The efficiency of core components including laser transmitters, atmospheric transmission channels and single triple-junction GaAs cells has approached their theoretical limits with very limited optimization space, while the efficiency of PV arrays integrated by individual cells is far below the ideal efficiency of single cells, which becomes the core bottleneck for system efficiency improvement[7-13]. Most existing studies focus on the external losses after array integration and the photoelectric response characteristics of single-junction GaAs cells, while systematic quantitative analysis on multi-size triple-junction GaAs cells for array integration under the coupled effects of multiple operating parameters remains insufficient.

In this study, the same batch of triple-junction GaAs PV cells intended for array integration were selected as the research object. Cells with three typical sizes were systematically tested under different standard laser incident intensities and typical operating temperatures, to obtain the complete I-V-P characteristics. To verify the feasibility and application value of this work, we quantified the conversion efficiency boundaries of individual cells before array integration under different working conditions, established an effective cell identification method that meets the current matching requirements of array integration, clarified the performance consistency level of the same batch of cells, and elucidated the decisive effect of individual cell photoelectric performance on the overall efficiency of PV arrays. This research provides a solid theoretical and experimental basis for the efficiency improvement of LWPT systems.

## Experimental setup

Figure 1 is the schematic diagram of the built longitudinal LWPT test platform. It consists of a laser driver, an 808 nm laser diode, a beam shaping system, a triple-junction GaAs PV cell, a temperature control unit and a data acquisition unit. The laser power can be adjusted by varying the input current of the driver, the beam shaping system homogenizes and collimates the laser beam, the PV cell converts laser energy into electrical power, the temperature control unit regulates the cell temperature, and the data acquisition unit records the output characteristics of the cell.

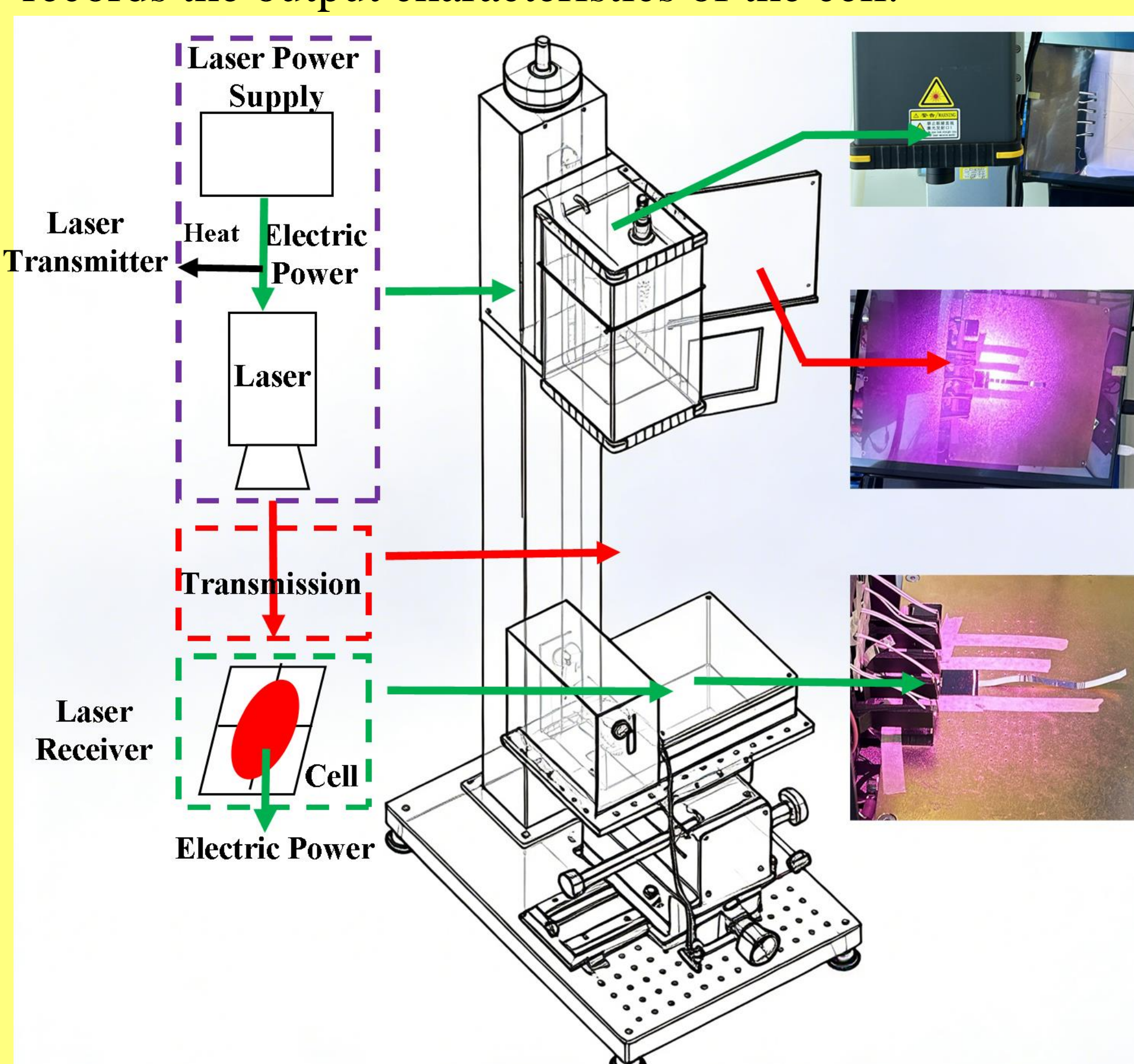


Fig. 1. Schematic diagram of the experimental platform

The PV cell holder is fabricated with a copper substrate of high electrical and thermal conductivity, which serves as the positive electrode of the cell backplane to ensure reliable electrical contact and efficient heat transfer. One side of the copper holder is connected to an intelligent constant-temperature device via water tubes to maintain the cell operating temperature, and the other side is connected to a data logger for accurate data acquisition. The bottom of the holder is designed as a three-dimensional adjustable stage with X/Y translation and tilt adjustment, to ensure the laser beam is perpendicular to the cell surface and precisely strikes the cell center, improving the consistency and reproducibility of experimental data. The testing procedure for each individual cell is carried out as follows. First, the edge positioning mechanism of the vacuum suction holes on the copper substrate is adjusted according to the actual cell dimensions, to precisely match the cell contour. Then, the positioning mechanism of the negative contact probe is calibrated to ensure the probe tip fully coincides with the negative electrode conductive layer on the cell surface, and the contact pressure is dynamically adjusted via a spring mechanism to achieve stable electrical contact.

In the experiment, a dynamic test program is executed through the software interface to scan the I-V and P-V characteristic curves of the cell, while synchronously monitoring the drift of the laser spot position and the variation of contact resistance during the test.

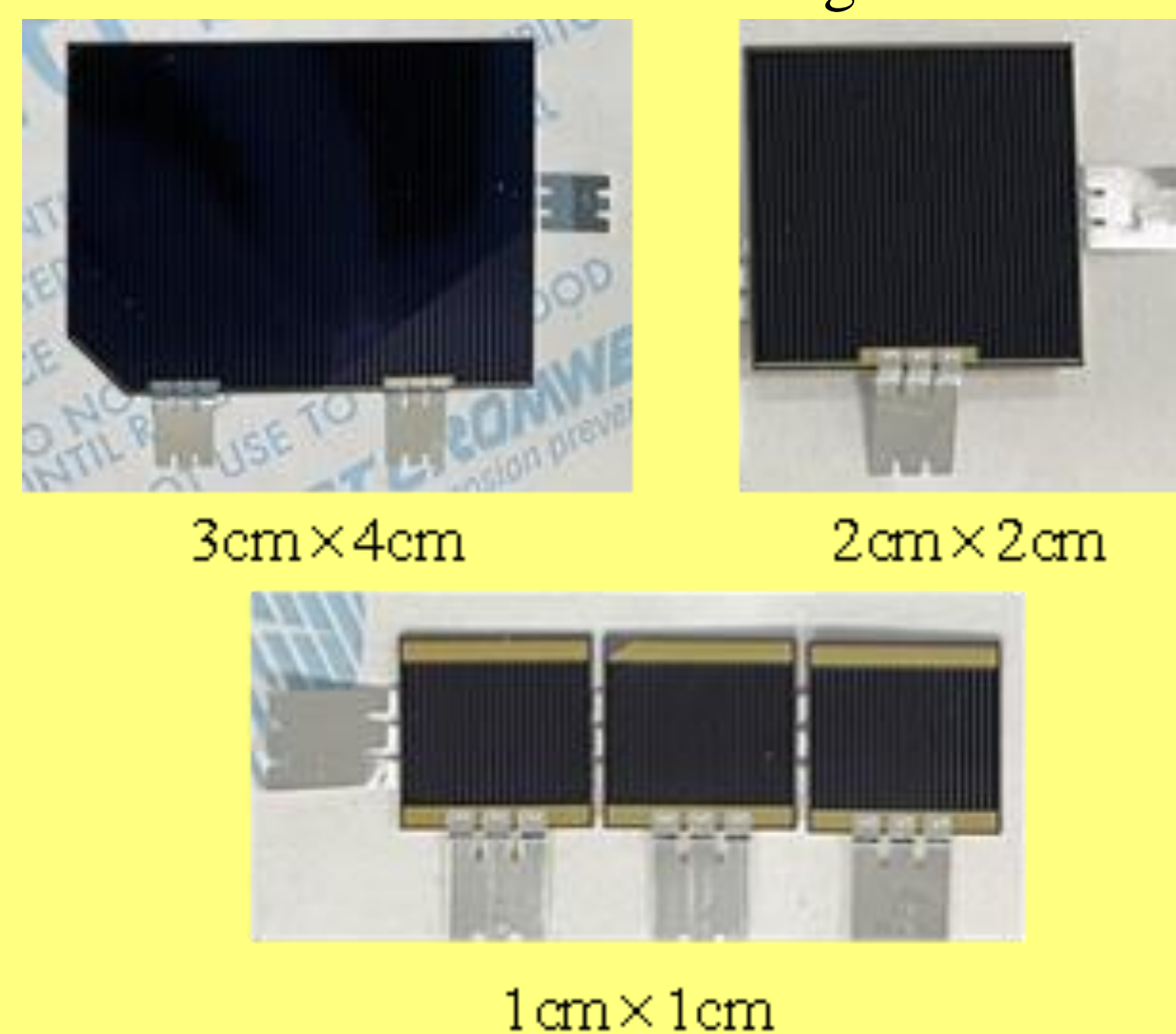


Fig. 2. Three-junction GaAs laser physical picture

The triple-junction GaAs PV cells used in this study were provided by the Shanghai Institute of Space Power-Sources. A photograph of the cells is shown in Figure 5. The cells were fabricated in three different sizes:  $1 \times 1 \text{ cm}^2$ ,  $2 \times 2 \text{ cm}^2$ , and  $3 \times 4 \text{ cm}^2$ .

## Experiment / Results

Performance benchmarks for triple-junction GaAs PV cells of different sizes were established to provide a reference for analyzing the cell characteristics under various light intensities and temperatures. Fig. 3 shows the full I-V and P-V characteristic curves of cells of three sizes ( $1 \times 1 \text{ cm}^2$ ,  $2 \times 2 \text{ cm}^2$ , and  $3 \times 4 \text{ cm}^2$ ) from the same batch under standard laser irradiance. The results presented in the figure indicate that the  $V_{oc}$  of the triple-junction GaAs PV cells remains stable in the range of 3.1–3.25 V across different cell sizes. This stability in  $V_{oc}$  can effectively reduce the number of series connections required in the array of an LWPT system and mitigate the associated current mismatch losses. Comparison of the output characteristic curves of cells with different sizes shows that the peak PCE of the  $3 \times 4 \text{ cm}^2$  and  $2 \times 2 \text{ cm}^2$  cells were 47.34% and 43.97%, respectively, with both exhibiting FF exceeding 80%. This indicates that the performance variability among cells was significantly reduced, and the intra-batch consistency was substantially superior to that of the smaller  $1 \times 1 \text{ cm}^2$  cells (which exhibited a mean efficiency of 30.5% and a mean FF of 64%).

Using the criteria that the deviation of  $I_{sc}$  for cells from the same batch should be within  $\pm 5\%$  and the photoelectric conversion efficiency should not be lower

than 90% of the batch average, the performance consistency of individual cells from the same batch was evaluated through sampling. The results show that among the seven  $1 \times 1 \text{ cm}^2$  cells from the same batch, five were identified as effective cells, corresponding to a yield of 71.4%; among the ten  $2 \times 2 \text{ cm}^2$  cells from the same batch, eight were effective cells, corresponding to a yield of 80%; among the eight  $3 \times 4 \text{ cm}^2$  cells from the same batch, seven were effective cells, corresponding to a yield of 87.5%. These results indicate that medium-to-large-area cells exhibit superior intra-batch consistency and higher yields, which can further reduce the probability of array mismatch and lower screening costs.

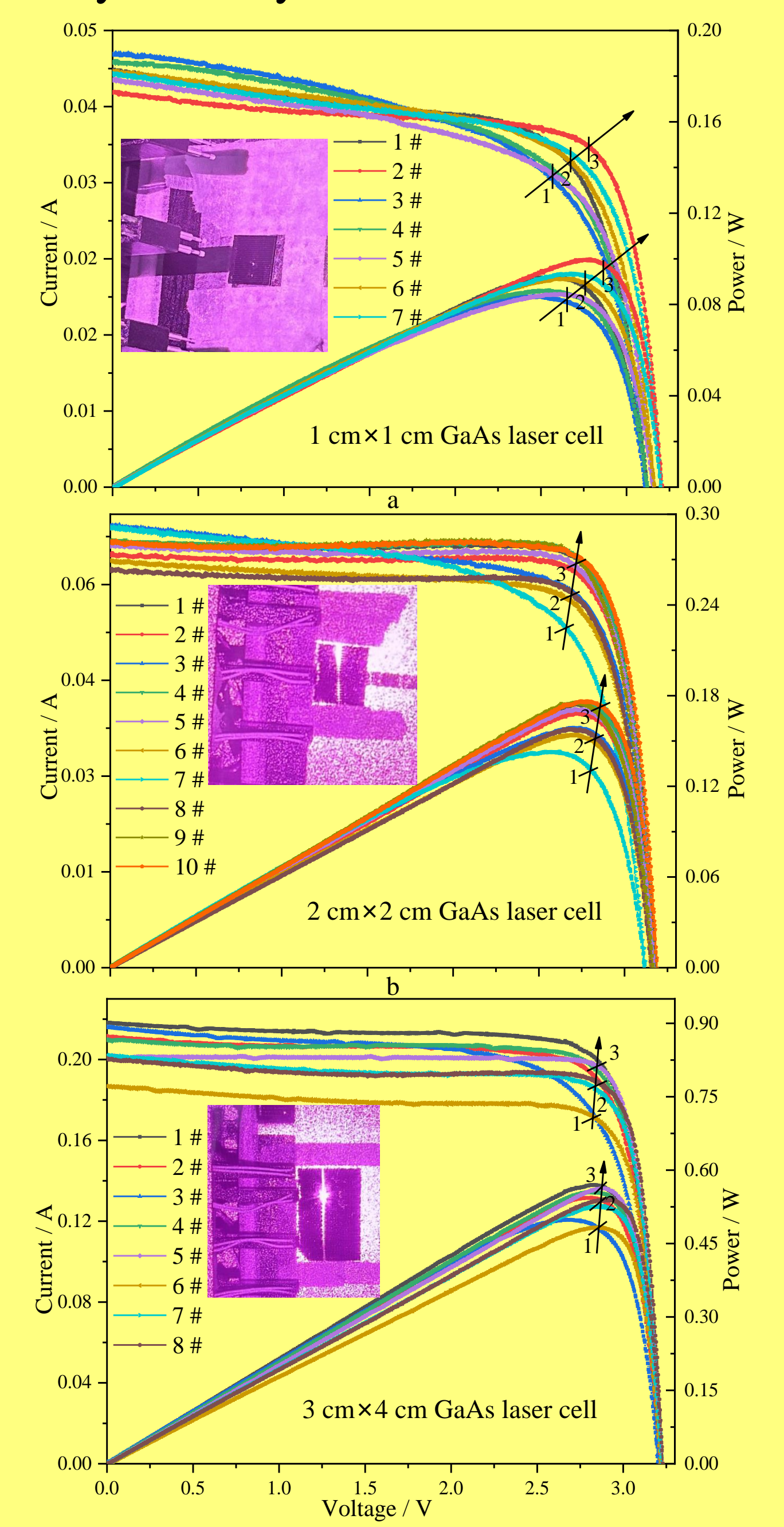


Fig. 3. Characteristics of triple-junction GaAs PV cells under standard laser irradiance.

## Conclusions

The main conclusions drawn from this study are as follows:

1. Under standard irradiance, cell  $V_{oc}$  stabilized at 3.10–3.25 V; PCE, FF and intra-batch consistency showed significant size dependence, with effective cell yield for array integration rising from 71.4% to 87.5% with increasing cell size.

2. Within 0.1–0.8 W/cm<sup>2</sup> incident intensity, cell peak PCE reached 51.65% at 3×standard irradiance, remained above 46% at 8× high irradiance, with intra-batch efficiency fluctuation of only 4.8 percentage points.

3. In 17–49 °C test range, total cell PCE degradation was only about 4 percentage points, FF stayed above 77%, and cells showed excellent temperature uniformity and operational stability without local hot spots.

## References

- [1] A. Mohammadnia, B.M. Ziapour, H. Ghaebi, M.H.J.O. Khooban, L. Technology, Feasibility assessment of next-generation drones powering by laser-based wireless power transfer, 143 (2021) 107283.
- [2] M. Ruan, X. Wang, W. Xu, M. Wang, P. Chen, J.J.E. Chen, The State of the Art of Research on Power Supply Technologies for Moving Targets, 18(5) (2025) 1174.
- [3] X. Li, G. Huang, Z. Wang, B.J.S.C.I.S. Zhao, Optics-driven drone, 67(2) (2024) 124201.
- [4] Z. Liu, T. Li, S. Li, C.C.J.N. Mi, Advancements and challenges in wireless power transfer: A comprehensive review, 1(2) (2024).
- [5] A.S.I. Al-Ezzi, M.J.J.o.t.K.P.S. Ansari, Analytical modelling and performance study of single-junction GaAs-based solar cell efficiency, 86(3) (2025) 245-262.
- [6] K. Jin, W.J.I.T.o.P.E. Zhou, Wireless laser power transmission: A review of recent progress, 34(4) (2018) 3842-3859.
- [7] G.P. Forcade, D.P. Wilson, M.N. Beattie, C. Pellegrino, H. Helmers, R.F. Hunter, O. Höhn, D. Lackner, L.-P. St-Arnaud, T.N.J.C.R.P.S. Tibbitts, Multi-junction laser power converters exceeding 50% efficiency in the short wavelength infrared, 6(6) (2025).
- [8] D. Li, L. Guo, H. Tan, G. Zhong, J. Wang, T. Li, H. Meng, Y. Fu, Z. Wu, Z.J.O.L. Zhong, 808 nm laser diode with a stepped-structure heat sink for high-efficiency laser wireless power transmission, 51(6) (2026) 1638-1640.s.